Journal of Food Engineering 99 (2010) 276–283

Contents lists available at ScienceDirect

Journal of Food Engineering

journal homepage: www.elsevier.com/locate/jfoodeng

Mass transfer of water and volatile fatty acids in cocoa beans during drying

D. Páramo [a], P. García-Alamilla [b], M.A. Salgado-Cervantes [a], V.J. Robles-Olvera [a], G.C. Rodríguez-Jimenes [a], M.A. García-Alvarado [a,*]

[a] Chemical and Biochemical Engineering Department, Instituto Tecnológico de Veracruz, Av. Miguel A. de Quevedo 2779, 91860 Veracruz, Mexico
[b] Food Engineering Department, Universidad Juárez Autónoma de Tabasco, Carretera Villahermosa-Teapa Km. 25, Col. La Huasteca, Villahermosa, Tabasco, Mexico

ARTICLE INFO

Article history:
Received 10 December 2009
Received in revised form 24 February 2010
Accepted 27 February 2010
Available online 9 March 2010

Keywords:
Cocoa beans
Drying
Volatile fatty acids
Mass transfer
Ellipsoidal cylindrical coordinates

ABSTRACT

In order to elucidate the phenomena involved in the remnant acidity of cocoa beans dried artificially, the diffusivities of water, and volatile fatty acids (VFAs: acetic, propionic, butyric and iso-butyric acids) in cocoa beans during drying were evaluated. Experimental drying kinetics of the acids were conduced at 40–60 °C with and without shell. Samples were taken at different drying times for moisture and acids content evaluation. VFAs content was evaluated by GC in a methanolic extract, and moisture content by a vacuum oven. Mass diffusivity was estimated from the fitting of experimental kinetics to a theoretical model that takes into consideration the beans' shape. Acetic, propionic and butyric acids diffusivities were significantly ($p < 0.05$) smaller than water diffusivities both with and without shell. VFAs diffusivities were between 1/6 and 1/22 diffusivities values for water. Iso-butyric acid diffusivity was not statistically significant but the value was smaller than for the other VFAs. The diffusivities of VFAs may explain the remnant acidity in artificially dried cocoa beans.

© 2010 Elsevier Ltd. All rights reserved.

1. Introduction

Volatile fatty acids (VFAs) have an important role on the development of essential flavor precursors during fermentation of cocoa beans (Faborode et al., 1995; Brito et al., 2000). Their content must be reduced during the subsequent drying process because elevated concentrations of these VFAs may be detrimental to cocoa products quality (García-Alamilla et al., 2007). Traditionally, cocoa beans are sun dried, but artificial convective drying has been introduced by Asian (Faborode et al., 1995) and Latin American (García-Alamilla et al., 2007) producers. However, experimental evidence has proved that during artificial drying the VFAs are not reduced at the same level that during sun drying, and therefore the artificially dried cocoa beans contain higher acidity (Jinap et al., 1994; Faborode et al.,1995; García-Alamilla et al., 2007). Since this higher acidity was found in convective drying which occurs at greater rate than sun drying, it is probability the result of a slower VFAs transfer with respect to water, or could be attributed to the increment in the mass transfer resistance of the cocoa beans shell during drying. García-Alamilla et al. (2007) developed a mathematical model for the heat and mass transfer of moisture and acidity in cocoa beans that takes into account both water and acidity diffusivities, as the mass transfer resistance in the shell. This model can be used for the search of adequate drying conditions that reducing the VFA concentration during convective drying. However, the proper application of such model requires the knowledge of the average diffusivity in cocoa beans and the mass transfer resistance in the shell, for both moisture and VFAs. Although there are reports on water and acidity mass transfer during cocoa beans drying, we have not found studies on the mass transfer of VFAs as individual compounds. As an example, Augier et al. (1999) evaluated the mass transfer of moisture and global acidity on cocoa beans during drying from punctual concentrations in different layers within beans; while Hii et al. (2009) evaluated water diffusivity by fitting the experimental average concentration to the analytical solution of Fick's second law in spherical coordinates. The mass transfer properties of VFAs as individual compounds require their identification, in this case by literature reports. The main VFA produced during cocoa fermentation is acetic acid (Brito et al., 2000) but there is evidence of the presence of propionic, butyric, iso-butyric and iso-valeric acids (Jinap et al., 1994).

Therefore, in this study the drying kinetic for moisture content, acetic, propionic, butyric, iso-butyric and iso-valeric acids concentrations were monitored in cocoa beans with and without shell. From the drying kinetics without shell the shell mass transfer resistance can be deduced. Since coca beans have ellipsoidal cylindrical shape, a theoretical discussion on a simple way to consider this shape for diffusivity estimation was presented.

2. Theoretical analysis

Hii et al. (2009) assumed cocoa beans may be described as spheres, however Augier et al. (1999) and García-Alamilla et al.

* Corresponding author. Fax: +52 2 934 57 01.
E-mail address: miguelg@itver.edu.mx (M.A. García-Alvarado).

0260-8774/$ - see front matter © 2010 Elsevier Ltd. All rights reserved.
doi:10.1016/j.jfoodeng.2010.02.028

Nomenclature

a	focal distance of ellipsoidal coordinates, m
C_p	specific heat of cocoa beans, J kg^{-1} K^{-1}
D	effective diffusivity in cocoa beans, m^2 s^{-1}
$\mathbf{e}_\phi$	unit vector basis for ϕ, normal to interface
k	heat conductivity in cocoa beans, W m^{-1} K^{-1}
k_c	mass transfer coefficient at interface, m s^{-1}
K	constant
m	experimental slope, s^{-1}
l	characteristic length for diffusion, m
h	heat transfer coefficient at interface, W m^{-2} K^{-1}
p	pressure, P
p	probability
r	short cylinder radius, m
$s^2(m)$	estimated variance of m
t	time, s
$t_{1-p/2(\upsilon)}$	t-student distribution, υ degree freedom
T	temperature, K
w	sample mass, kg
x, y, z	rectangular coordinates, m
X	dry basis concentration in cocoa beans, kg kg^{-1}
Y	dry basis concentration in air, kg kg^{-1}
Greeks	
ε	shell thickness, m
μ, v	ellipsoidal coordinates, m
ϕ	thermodynamic activity
λ^2	eigenvalue
ρ	density, kg m^{-3}
τ	dimensionless time (Fourier number)
ΔH	latent evaporation heat, J kg^{-1}
Ψ	dimensionless moisture
Sub indexes	
0	at initial or reference
a	in air
cyl	for short cylinder
d	for dried compounds
e	at equilibrium
i	at interface
cyl	for cylinder
ell	for ellipsoidal cylinder
scy	for short cylinder
w	for water
β	in cocoa beans
ω	for any compound

(2007) stated that a plane sheet is more approximate to describe the beans geometry. Rigorously, the cocoa beans shape is better described like an ellipsoidal cylinder, as it can be depicted in Fig. 1. The ellipsoidal cylindrical coordinates (μ, v, z) represented in Fig. 2 are related with rectangular coordinate by Eq. (1),

$$\left.\begin{aligned} x &= a\cosh(\mu)\cos(v) \\ y &= a\sinh(\mu)\sin(v) \\ z &= z \end{aligned}\right\} \tag{1}$$

for $\mu \geqslant 0$, $0 \leqslant \upsilon \leqslant 2\pi$, and $-\infty < z < \infty$

Under this geometry, the mass transfer of any compound (ω): water or some VFA) during cocoa drying is represented by Fick's second Law as follows,

$$\frac{\partial X_\omega}{\partial t} = \frac{\frac{\partial}{\partial \mu}\left(D_\omega \frac{\partial X_\omega}{\partial \mu}\right) + \frac{\partial}{\partial \upsilon}\left(D_\omega \frac{\partial X_\omega}{\partial \upsilon}\right)}{a^2(\sinh^2\mu + \sin^2\upsilon)} + \frac{\partial}{\partial z}\left(D_\omega \frac{\partial X_\omega}{\partial z}\right)$$
$$\text{in } 0 \leqslant z \leqslant l_z,\ \ 0 \leqslant \mu \leqslant l_\mu,\ \ 0 \leqslant \upsilon \leqslant 2\pi,\ \ t \geqslant 0 \tag{2}$$

At the center of the cocoa beans ($z = 0,\ \mu = 0$) the symmetry produces,

$$\frac{\partial X_\omega}{\partial z} = 0 \quad \text{at } z = 0 \tag{3a}$$

$$\frac{\partial X_\omega}{\partial \mu} = 0 \quad \text{at } \mu = 0 \tag{3b}$$

Water or VFAs evaporate at the beans surface in contact with drying air. This surface is the bean–air interface, which under the geometry applied occurs in $z = l_z$ and $\mu = l_\mu$. Therefore the interface equations are written in terms of diffusivity in beans side, and convective mass transfer in air side. That is,

$$-D_\omega \rho_{d\beta} \frac{\partial X_{\omega i}}{\partial z} = k_c \rho_{da}(Y_{\omega i} - Y_\omega) \quad \text{at } z = l_z \tag{4a}$$

$$-\frac{D_\omega \rho_{d\beta} \frac{\partial X_{\omega i}}{\partial \mu}}{a\sqrt{\sinh^2\mu + \sin^2\upsilon}} = k_c \rho_{da}(Y_{\omega i} - Y_\omega) \quad \text{at } \mu = l_\mu \tag{4b}$$

In order to represent the third elliptical cylindrical coordinate, it is necessary to observe that the unit vector of direction υ is orthogonal to the surface normal, as can it be observed in Fig. 2, and evaporation is assumed normal to the beans surface. Therefore, in agreement with elliptic cylindrical coordinates there is not a source for concentration gradient in υ direction, which means that,

Fig. 1. Cocoa beans shape at the end of drying.

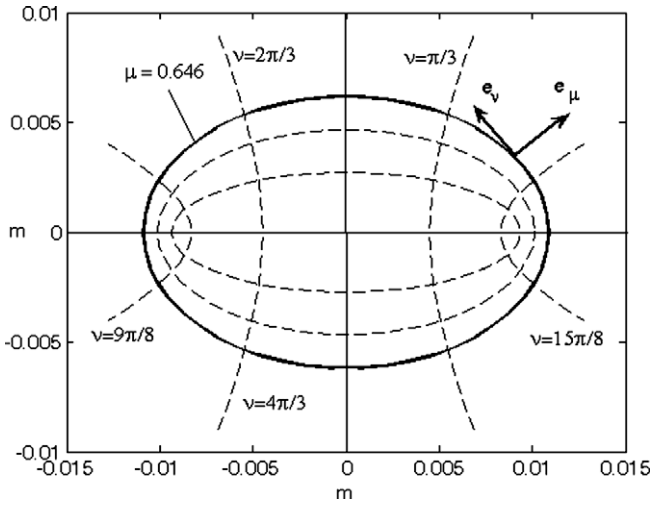

Fig. 2. Ellipsoidal cylindrical coordinates.

$$-\frac{D_\omega \rho_{d\beta} \frac{\partial X_{\omega i}}{\partial \upsilon}}{a\sqrt{\sinh^2\mu+\sin^2\upsilon}} = 0 \quad \text{in } 0 \leqslant \upsilon \leqslant 2\pi \text{ at } \mu = l_\mu \text{ and } z = l_z \tag{5}$$

Additionally, at the bean–air interface, the water and VFA are assumed in mass equilibrium between the bean and air,

$$X_{\omega i} = f(Y_{\omega i}, T_i) \tag{6}$$

Eqs. (2), (3a), (3b), (4a), (4b), (5) describe the mass transfer during cocoa beans drying, and are strongly dependent of the effective diffusivity (D_ω) of the transported compound. Effective diffusivity as the result of molecular diffusion and the microstructure of the medium must be a temperature function. In Bird et al. (1960) can be found theoretical relationships between molecular diffusion and temperature both in gas phase (Chapman–Enskog equation) and liquid phase (Stoke–Einstein equation). Therefore, the heat transfer equations are required to complete the mathematical description of the process. Fourier law expressed in ellipsoidal cylindrical coordinates describes the heat transfer conduction,

$$\frac{\partial C_p \rho_\beta T_\beta}{\partial t} = \frac{\frac{\partial}{\partial \mu}\left(k\frac{\partial T_\beta}{\partial \mu}\right) + \frac{\partial}{\partial \upsilon}\left(k\frac{\partial T_\beta}{\partial \upsilon}\right)}{a^2(\sinh^2\mu+\sin^2\upsilon)} + \frac{\partial}{\partial z}\left(k\frac{\partial T_\beta}{\partial z}\right)$$
$$\text{in } 0 \leqslant z \leqslant l_z,\ \ 0 \leqslant \mu \leqslant \varphi_\mu,\ \ 0 \leqslant \upsilon \leqslant 2\pi,\ \ t \geqslant 0 \tag{7}$$

$$\frac{\partial T_\beta}{\partial z} = 0 \quad \text{at } z = 0 \tag{8a}$$

$$\frac{\partial T_\beta}{\partial \mu} = 0 \quad \text{at } \mu = 0 \tag{8b}$$

In the case of heat transfer, is necessary to take into consideration the amount of heat required to evaporate water and VFA. Therefore, and assuming that interface temperature (T_i) is the same for beans and air, the interfacial heat transfer in the air–beans interface is,

$$-k\frac{\partial T_i}{\partial z} = h(T_i - T_a) - \sum_\omega k_c \rho_{da}(Y_{\omega i} - Y_\omega)\Delta H_\omega \text{ at } z = l_z \tag{9a}$$

$$-\frac{k\frac{\partial T_i}{\partial \mu}}{a\sqrt{\sinh^2\mu+\sin^2\upsilon}} = h(T_i - T_a) - \sum_\omega k_c \rho_{da}(Y_{\omega i} - Y_\omega)\Delta H_\omega \text{ at } \mu = l_\mu \tag{9b}$$

$$-\frac{k\frac{\partial T_i}{\partial \upsilon}}{a\sqrt{\sinh^2\mu+\sin^2\upsilon}} = 0 \quad \text{in } 0 \leqslant \upsilon \leqslant 2\pi \text{ at } \mu = l_\mu \text{ and } z = l_z \tag{10}$$

Eq. (2) describes the punctual concentration, for water or VFA, within the bean, but the concentration experimentally measured is the average concentration. This average concentration is obtained from the integral of punctual concentration (X_ω), obtained from Eq. (2), over the particle volume in the reference coordinates,

$$\bar{X}_\omega = \frac{\int_0^{l_z}\int_0^{l_\mu}\int_0^{2\pi} a^2(\sinh^2\mu+\sin^2\upsilon)X_\omega d\upsilon d\mu dz}{\int_0^{l_z}\int_0^{l_\mu}\int_0^{2\pi} a^2(\sinh^2\mu+\sin^2\upsilon)d\upsilon d\mu dz} \tag{11}$$

Eq. (11), as the integral result of Eqs. (2), (3a), (3b), (4a), (4b), (5), (6), (7), (8a), (8b), (9a), (9b), (10), defines the average concentration ($\bar{X}_\omega$) of water or any VFA within of cocoa beans at any time during drying, and therefore may be used for the diffusivity evaluation by fitting to experimental results. Although the diffusivity may be a moisture function due the microstructure changes during drying, it has been a common practice the evaluation of an average effective diffusivity of water between initial and final product moisture, since the early drying studies until today (Sherwood, 1929; Senadeera et al., 2003; Wang et al., 2007; Hii et al., 2009). A simple way to evaluate this effective diffusivity during drying is by fitting the average moisture kinetic experimentally obtained to the analytical solution of the mass transfer equations in the proper coordinate system, with some simplifications. The most common simplifications applied are: constant average effective diffusivity, constant size, constant product temperature and constant interface concentration in equilibrium with air. Even with these assumptions, the mass transfer equation in elliptic cylindrical coordinate system (Eq. (1) or (4)) has not a friendly analytical solution. Hernández-Díaz et al. (2008) proposed a method to evaluate average diffusivities in complex geometries. Under this method the kinetic of an average dimensionless moisture content ($\bar{\Psi}_\omega$) as function of Fourier number (τ), both defined in Eq. (12)

$$\bar{\Psi}_\omega = \frac{\bar{X}_\omega - X_{\omega e}}{X_{\omega 0} - X_{\omega e}} \qquad \tau = \frac{D_\omega t}{l^2} \tag{12}$$

was calculated with numerical solution of heat and mass transfer equations, equivalents to Eqs. (2), (3a), (3b), (4a), (4b), (5), (6), (7), (8a), (8b), (9a), (9b), (10), (11) in the proper geometry. The obtained kinetics exhibits an asymptotic linear behavior up to a given value of Fourier number. In this linear zone the drying kinetic may be represented by,

$$\bar{\Psi}_\omega = Ke^{-\lambda^2\tau} \tag{13}$$

Eq. (13) plotted in a semi-log scale is linear with slope λ^2, called theoretical slope. Therefore, the linear zone of average dimensionless moisture as function of time obtained from experimental drying kinetics may be represented by,

$$\bar{\Psi}_\omega = Ke^{-mt} \tag{14}$$

where the experimental slope (m) may be calculated with linear regression of the linear zone of experimental drying kinetic in a semi-log scale. Like Eqs. (13) and (14) represent the same phenomenon, the following expression is obtained,

$$m = -\frac{\lambda^2 D_\omega}{l^2} \tag{15}$$

Eq. (15) is a way to calculate the average effective diffusivity from: experimental slope of drying kinetics; the theoretical slope from dimensionless drying kinetic at a given geometry; and the characteristic length for diffusion.

In the case of Hernández-Díaz et al. (2008) the given geometry was represented by a prolate coordinate system. In order to generalize the described method for any geometry represented by an orthogonal coordinate system, a theoretical dissertation is depicted in Appendix. The results of Appendix dissertation demon-

strates that upon validity of Eq. (12), λ^2 depends only of the product shape, the effects of diffusivity and product characteristic length are manifested in the Fourier number (τ), and the transitory effects of temperature are manifested in constant K.

3. Materials and methods

3.1. Experimental drying experiments

Fermented cocoa beans were obtained from a local cocoa producer in Tabasco (México). Beans were dried in a fixed bed dryer (Apex mod. SSE65) at different conditions. Experimental drying kinetics were obtained at two temperatures (40 and 60 °C), two air velocities (0.5 and 2 m/s), with and without shell following a $2 \times 2 \times 2$ factorial design. Each one of the 2^3 design treatments consisted in several samples of 15–20 beans, which were dried at a given time, in a monolayer placed in the dryer chamber, and then the complete sample was analyzed for size, moisture and VFA. Beans size was measured with a vernier. Kinetic data were obtained with independent samples and all experiments were carried out in duplicate. The moisture content was evaluated, by duplicate, in a vacuum oven at 105 °C until constant weight.

3.2. Moisture and volatile acids determination

The VFAs were extracted in methanol using an ultrasonic bath and results were compared to the Mothe-Efter extraction method. Extraction took place in an ultrasonic bath (Westprime Systems mod. LR84943). Approximately 500 mg of the drying kinetic samples were frozen in liquid nitrogen, and powdered in a mortar. The powder was placed into a 125 mL screw-cap Erlenmeyer flask (Pyrex), and approximately 10 mL of methanol were added. Sonication of the mixture was carried out for 30 min at 25 °C, then the homogenate was through with Whatman No. 4 filter paper and then with 0.45 μm filter unit and analyzed by GC. The GC system (Varian 3900 GC, California, USA) was equipped with an auto sampler (Varian CP-8400), an auto injector (Varian CP-8410). The detector used was FID. The column flow rate was 5 mL/min (Nitrogen as carrier gas), and the split ratio was 1:100. A CP-Wax 57 CB column from Varian (50 m × 0.32 mm ID × 0.2 μm film thickness) was used for the separation. The program started at 70 °C for 5 min, followed by a temperature ramp of 4 °C/min until 160 °C and held for 2 min. Injector and detector were kept at 230 and 250 °C, respectively. The sample volume injected was 1 μL. The amounts of volatile acids were calculated, as mg volatile acid per kg cocoa beans, by using an external calibration curve, which were obtained for each volatile acid standard. The analyses were performed in triplicate. Acetic, propionic, butyric, iso-butyric and *n*-valeric acids (98–99%) standards were purchased from Sigma–Aldrich (St. Louis, MO). Solvents (methanol and distilled water) were HPLC grade and purchased from J.T. Baker.

3.3. Model solution

In order to obtain the theoretical slope λ^2 of Eq. (13), Eqs. (2), (3a), (3b), (4a), (4b), (5)–(7), (8a), (8b), (9a), (9b), (10), (11) were solved numerically. Space derivatives of Eqs. (2), (3a), (3b), (4a), (4b), (5)–(7), (8a), (8b), (9a), (9b), (10), (11) were substituted by first order finite differences. This procedure produces a set of ordinary differential equations that can be solved by the method Runge–Kutta. The average moisture in the beans (Eq. (11)) was calculated with 3D trapezoidal rule. The characteristic length of diffusion (l) was taken as the half of the beans thickness, represented by l_z in Eq. (2).

3.4. Diffusivities evaluation

The water and VFA average effective diffusivities were evaluated with Eq. (15) from experimental drying kinetics and the theoretical slope (λ^2). Experimental slope (m) was calculated with linear regression of the log of dimensionless concentration vs. time. The characteristic length (l) was taken as the half of cocoa beans thickness. Equilibrium moisture (X_e) required in the calculation of dimensionless moisture was estimated from cocoa sorption isotherms reported in the literature (García-Alamilla et al., 2007),

$$\varphi_w = 1 - e^{-100.17X_{wi}^{1.939}} \tag{16}$$

and equilibrium concentrations for VFA were taken as zero because the drying air has no VFA vapors.

Both goodness of the fit and the dispersion of experimental slope calculated with linear regression were evaluated with the $(1-p)\times 100\%$ confidence interval for the experimental slope. The following well-known statistic relation was used,

$$m \pm t_{1-p/2(v)}\sqrt{s^2(m)} \tag{17}$$

where the estimator variance ($s^2(m)$) was calculated from design matrix and the square sum of residuals of model fitted as follows (Seber and Wild, 1989),

$$s^2(m) = \frac{\sum_{i=1}^{n}(\ln(\bar{\Psi}_{\omega experimental})_i - \ln(\bar{\Psi}_{\omega predicted})_i)^2}{n-1}\delta_{22}$$

where n is the number of kinetic experimental points considered, and δ_{22} is the second diagonal element of the matrix $(\mathbf{D}'\mathbf{D})^{-1}$ in which $\mathbf{D}$ is the design matrix defined as,

$$\mathbf{D} = \begin{bmatrix} \frac{\partial \ln(\bar{\Psi}_{\omega predicted})_1}{\partial K} & \frac{\partial \ln(\bar{\Psi}_{\omega predicted})_1}{\partial m} \\ \cdot & \cdot \\ \cdot & \cdot \\ \frac{\partial \ln(\bar{\Psi}_{\omega predicted})_n}{\partial K} & \frac{\partial \ln(\bar{\Psi}_{\omega predicted})_n}{\partial m} \end{bmatrix}$$

If the zero value is not contained in a 95% confidence interval (17) indicates that the probability of dispersion would be greater than the estimated parameter value is less than 5%, and therefore the model fitting and the experimental slope would be statistically significant.

4. Results

4.1. Cocoa beans characterization

Average size of cocoa beans during drying are listed in Table 1. As expected, due the shell thickness, the beans without shell are barely smaller (and not statistically significant) than with shell. However the shell has a protective effect of the bean during drying, as can be observed in Fig. 1. Beans without shell browned at the end of drying. Another fact to consider for mass transfer calculations is bean shrinkage, which is significant during drying (Table 1). Therefore, the characterization of beans in elliptic cylindrical coordinates was made with the sizes at the middle of drying. Beans characteristics dimensions were the focal distance a, the representative perimeter l_μ and the half of thickness l_z, that approximate the beans size and shape. These dimensions were estimated from the half of major axis and minor axis sizes according to Eq. (1). l_z was the half of average cocoa beans thickness at the middle of drying, and this size was taken as the characteristic length for diffusion (l). The values obtained, both with and without shell, are listed in Table 1, and they were used in the numerical solution of Eqs. (2), (3a), (3b), (4a), (4b), (5)–(7), (8a), (8b), (9a), (9b), (10), (11)

Table 1
Cocoa beans size and elliptic cylindrical coordinate characterization.

Size	Cocoa beans with shell during drying (cm)			Cocoa beans without shell during Drying (cm)		
	Initial	Medium[b]	Final[c]	Initial	Medium	Final
(Mayor axis)/2	1.19 ± 0.03 [a]	1.09 ± 0.03	1.08 ± 0.03	1.19 ± 0.03	1.03 ± 0.03	1.00 ± 0.03
(Minor axis)/2	0.68 ± 0.03	0.62 ± 0.02	0.62 ± 0.02	0.68 ± 0.03	0.60 ± 0.01	0.59 ± 0.03
Thickness/2	0.47 ± 0.03	0.30 ± 0.02	0.29 ± 0.02	0.47 ± 0.02	0.33 ± 0.02	0.32 ± 0.02
l_μ Average		0.646			0.666	
$l_z = l$ Average		0.30			0.33	
a Average		0.9			0.84	
λ^2		4.347			5.512	

[a] The dispersion represent the 95% confidence interval.
[b] The medium of drying was 5 h at 60 °C and 15 h at 40 °C.
[c] The final of drying was 10 h at 60 °C and 30 h at 40 °C.

4.2. Model solution

Additionally to beans characteristic lengths in elliptical cylindrical coordinate, the numerical solution requires heat and mass transfer properties. As initial guess values for diffusivity, an equation was deduced from the Augier et al. (1999) cocoa drying data. The obtained equation was,

$$D = 10.23692e^{-7632.765/T}D \quad \text{in } m^2\ s^{-1},\ T \text{ in K},$$

The other properties were taken from García-Alamilla et al. (2007). These properties evaluated at cocoa beans average moisture between 0.76 and 0.10 g water g dry matter^{-1} are,

Properties at average beans moisture,

$$k = 0.3 \text{ in W m}^{-1}\text{ K}^{-1}, \quad C_p = 1700 \text{ in J}\cdot\text{kg}^{-1}\text{ K}^{-1},$$
$$\rho_{d\beta} = 700 \text{ in } kg\text{ m}^{-3}, \quad \rho_\beta = 1050 \text{ in kg m}^{-3}$$

Properties at average interface condition,

$$k_c = 0.006 \text{ in m s}^{-1}, \quad h = 30 \text{ in W m}^{-2}\text{ K}^{-1}$$

Air conditions and initial beans moisture,

$$Y = 0.01 \text{ g water (g dry air)}^{-1}, \quad T_a = 40 \text{ or } 60^\circ\text{C},$$

$$X_{w0} = 0.76 \text{ g water (g dry matter)}^{-1}$$

Interface mass equilibrium (Eq. (6)),$Y_{wi} = \frac{p_w^o \varphi_w / p}{1 - p_w^o \varphi_w / p} \frac{18}{28}$ where the water activity (φ_w) was calculated with Eq. (16).

Eqs. (2), (3a), (3b), (4a), (4b), (5)–(7), (8a), (8b), (9a), (9b), (10), (11) were numerically solved, as it was described in Section 3.3, for the beans characteristic length with and without shell (Table 1) and the properties listed above. The semi-log relationship between dimensionless average moisture (Ψ)) vs. Fourier number (τ) obtained with numerical solution is plotted in Fig. 3. It can be appreciated that the relation is linear at $\tau > 0.1$ which indicates that the solution has reached the asymptotic behavior (Eq. (13)). Under this behavior the slopes of Fig. 3 are independent of heat and mass transfer properties, as it was demonstrated in Appendix. Therefore the slopes of Fig. 3 are the theoretical ones (λ^2), which are listed in Table 1. An important comparison is the theoretical slope for a conventional geometry that approximates the shape of cocoa beans. By inspection of Fig. 1, this conventional geometry is a short cylinder. From the asymptotic behavior of the analytical solution of Fick's second law in rectangular and in cylindrical coordinates (Crank, 1975), the Eq. (13) may be written as,

$$\bar{\Psi}_\omega = Ke^{-[\frac{\pi^2}{4} + \lambda_{cyl}^2 (\frac{l_z}{r})^2]\tau} \tag{18}$$

where λ_{cyl} is the first root of $J_0(\lambda) = 0$ which value is $\lambda_{cyl} = 2.4048$, and r the cylindrical radius. Therefore the theoretical slope under this geometry is equal to,

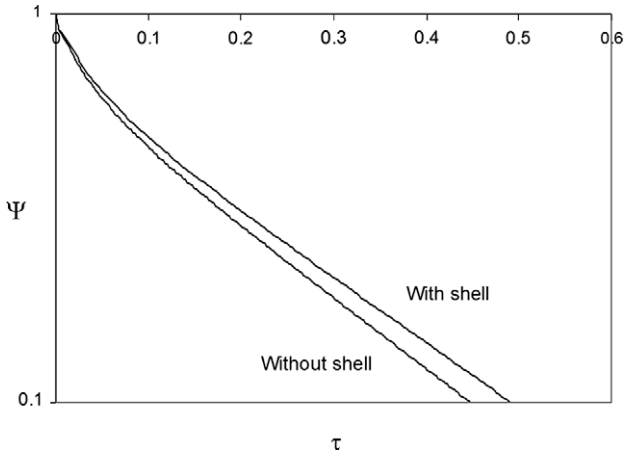

Fig. 3. Average dimensionless concentration of theoretical drying kinetic in ellipsoidal cylindrical coordinates with the size indicated in Table 1.

$$\lambda_{scy}^2 = \frac{\pi^2}{4} + \lambda_{cyl}^2 \left(\frac{l_z}{r}\right)^2 \tag{19}$$

In order to use Eq. (19) a cylindrical radius is necessary. The best approximation of the cocoa beans to a short cylindrical geometry is with the equivalent radius that produces a cylindrical surface equivalent to the ellipsoidal surface of the size reported in Table 1. Therefore the theoretical slopes under a short cylindrical geometry are,

With shell $\lambda_{scy}^2 = 3.238$ (equivalent radius $r = 0.822$ cm)

Without shell $\lambda_{scy}^2 = 3.487$ (equivalent radius $r = 0.786$ cm)

Finally, from Eq. (15), $\frac{D_{\omega\beta scy}}{D_{\omega\beta ell}} = \frac{\lambda_{ell}^2}{\lambda_{scl}^2}$ and applying the theoretical slopes of Table 1, the following ratios were obtained,

With shell $\frac{D_{\omega\beta scy}}{D_{\omega\beta ell}} = 1.343$

Without shell $\frac{D_{\omega\beta scy}}{D_{\omega\beta ell}} = 1.581$

That is, the effective diffusivity evaluated assuming the cocoa bean geometry as a short cylinder would be overestimated in around 1.5 times the effective diffusivity calculated with the ellipsoidal cylindrical coordinates which is a better approximation of the bean shape (Figs. 1 and 2).

Table 2
Cocoa beans initial moisture and VFA concentrations in g/g dm.

Beans state	Moisture	Acetic acid $\times 10^3$	Propionic acid $\times 10^3$	Butyric acid $\times 10^3$	Iso-butyric acid $\times 10^3$
With shell	1.27 ± 0.12[a]	25.51 ± 4.59	2.16 ± 0.33	2.37 ± 0.66	0.49 ± 0.05
Without shell	0.81 ± 0.07	13.72 ± 4.31	1.48 ± 0.21	1.34 ± 0.63	0.43 ± 0.05

[a] Dispersion represents the 95% confidence interval.

Table 3
Water and VFA diffusivities[a] in cocoa beans during drying.

Beans state	Moisture	Acetic acid	Propionic acid	Iso-Butyric acid	Butyric acid
With shell 40 °C	4.61 ± 0.55[b]	0.54 ± 0.36	0.30 ± 0.21	0.65 ± 0.98	0.50 ± 0.39
With shell 60 °C	8.00 ± 2.1	1.18 ± 0.56	0.34 ± 0.67	0.08 ± 1.04	0.85 ± 0.52
Without shell 40 °C	11.4 ± 2.0	1.36 ± 0.31	1.16 ± 0.50	1.14 ± 0.39	0.73 ± 0.41
Without shell 60 °C	21.5 ± 10.8	3.30 ± 1.48	2.48 ± 1.12	0.76 ± 0.79	1.54 ± 1.34

[a] Diffusivity $\times 10^{11}$ in $m^2\ s^{-1}$.
[b] Dispersion represent the 95% confidence interval calculated with Eq. (17).

4.3. Water and VFA experimental kinetics

Initial moisture and VFA obtained in the cocoa beans with and without shell are listed in Table 2. There is enough evidence ($p < 0.05$) that the beans with shell have greater concentrations of water and VFA than the beans without shell, which is expected because shell is in contact with the mucilage where the main fermentation changes occurs. The drying kinetics for water and VFAs are plotted in Fig. 4–8. It can be observed that the kinetic of water, acetic, propionic and butyric acids represented in a semi-log scale show an approximate linear trend one hour after of the drying beginning. Iso-butyric acid kinetic has the greatest dispersion probably because that this component concentration in beans was at the limits of detection.

The linear behavior was confirmed by fitting the experimental drying kinetics, at $t > 1$ h, to a linear model in semi-log scale, which results in the continuous lines plotted in Figs. 4–8. The slopes of these lines (m) and their 95% interval confidence limits (calculated with Eq. (17)) were applied in Eq. (15) jointly with their characteristic length ($l = l_z$) listed in Table 1, for the calculation of average diffusivities, and their confidence interval. The whole set of the results are listed in Table 3. All of the diffusivities were statistically significant (the zero value is not included in the 95% interval confidence), except those of the iso-butyric acid and one of the butyric acid, due to a high degree of dispersion in their kinetics (Figs. 7 and 8). This significance demonstrates that the Eq. (14), applied for $t > 1$ h, produces an explained variance bigger than the non-explained variance (dispersion), and therefore is statistic evidence ($p < 0.05$) that Eq. (14) represents adequately the drying kinetics. Additionally, the 95% interval confidence of diffusivities is evidence supporting that the shell produces a significant ($p < 0.05$) mass transfer resistance for water, acetic and propionic acids. This resistance can be appreciated by the greater diffusivities obtained for beans without shell at the two temperatures, and in Figs. 4–6 in which is evident that drying kinetics of water acetic and propionic acids are faster without shell. The reduction of diffusivities with shell was in the order of 1/3 to 1/9 with respect to diffusivities without shell. Therefore, the shell has a protective effect during drying and a significant mass transfer resistance for both water and VFAs. In the case of butyric and iso-butyric acids the dispersion of the results did not allow to draw a conclusion. Another fact is that after inspection of Figs. 4–8, there is not evidence that diffusivity decreases during drying. That is, the model with moisture independent diffusivity represents a feasible description of water and VFAs mass transfer.

One of the most relevant facts shown by the results listed in Table 3 is that acetic, propionic and butyric acids diffusivities are statistically ($p < 0.05$) smaller than the water diffusivity at the

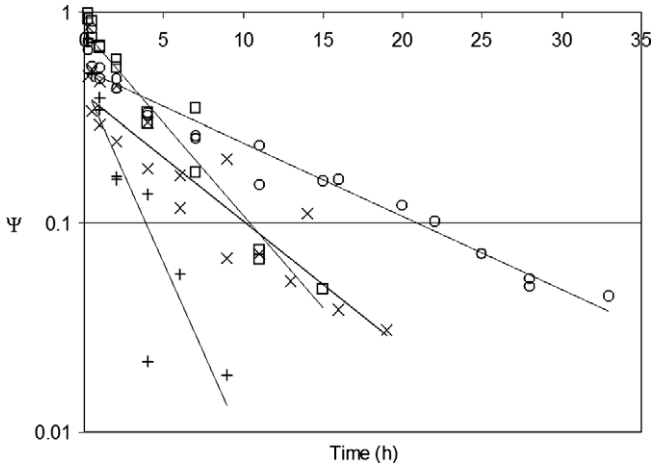

Fig. 4. Dimensionless moisture content drying kinetic of cocoa beans at 60 °C with shell (×), without shell (+), at 40 °C with shell (○) and without shell (□). Continuous lines were generated by Eq. (14) fitted to experimental data.

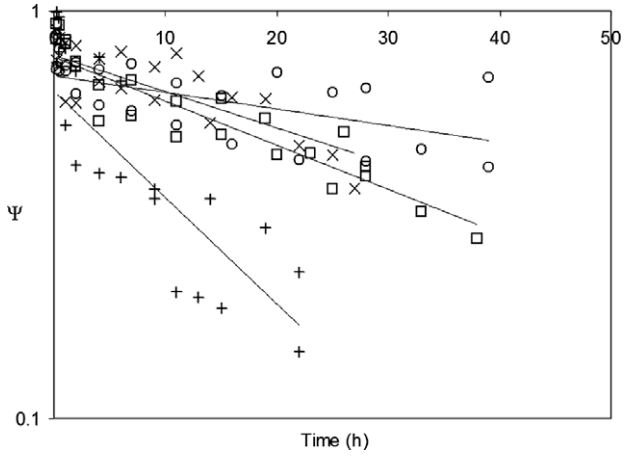

Fig. 5. Dimensionless acetic acid content drying kinetic of cocoa beans at 60 °C with shell (×), without shell (+), at 40 °C with shell (○) and without shell (□). Continuous lines were generated by Eq. (14) fitted to experimental data.

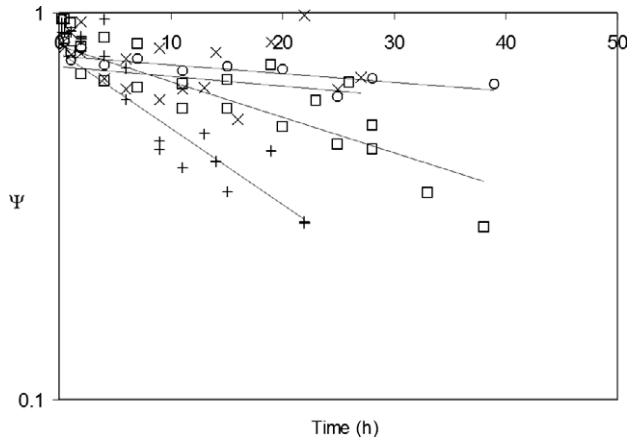

Fig. 6. Dimensionless propionic acid content drying kinetic of cocoa beans at 60 °C with shell (×), without shell (+), at 40 °C with shell (○) and without shell (□). Continuous lines were generated by Eq. (14) fitted to experimental data.

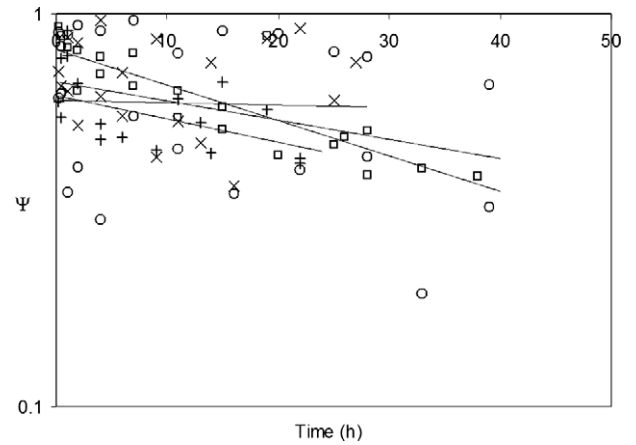

Fig. 7. Dimensionless iso-butyric acid content drying kinetic of cocoa beans at 60 °C with shell (×), without shell (+), at 40 °C with shell (○) and without shell (□). Continuous lines were generated by Eq. (14) fitted to experimental data.

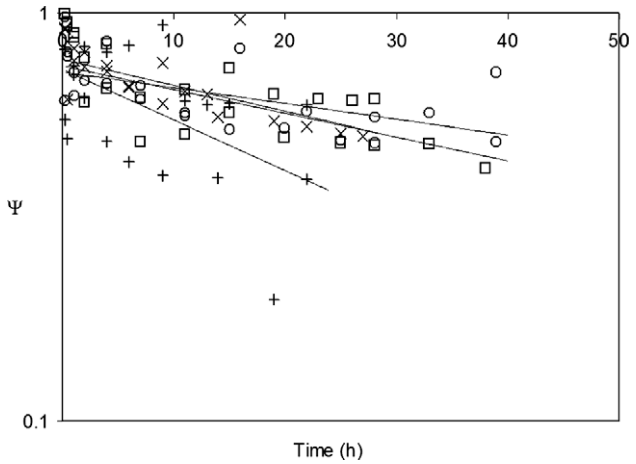

Fig. 8. Dimensionless butyric acid content drying kinetic of cocoa beans at 60 °C with shell (×), without shell (+), at 40 °C with shell (○) and without shell (□). Continuous lines were generated by Eq. (14) fitted to experimental data.

two temperatures and with or without shell. The VFAs diffusivities were between 1/6 and 1/22 of water diffusivity. This means that acidity lost during drying is ca. 10 times slower than moisture lost with or without shell. Therefore, in convective drying (with lower drying time than sun drying) there is the possibility of remnant acidity at the end of drying if the initial acidity concentration is high, only due to the different rates of mass transfer between water and VFAs.

The above conclusion leads on some solutions to avoid the high acidity in cocoa beans dried convectively. One of them, may be the cocoa bean convective drying by steps with stages without air flow that allow the internal rearrangement of acidity and water profiles. Another solution may be drying using air with controlled moisture that controls the water surface evaporation. In any case, the optimal operation conditions: air flow, number and duration of stages, air moisture and temperature; can be found applying Table 3 diffusivities in a drying simulator like the reported by García-Alamilla et al. (2007).

5. Conclusion

In this study it was shown that although the shell represents a mass transfer resistance for moisture and VFAs, the remnant acidity in convectively dried cocoa beans is probably the result of the smaller diffusivities of VFAs with respect to water. The diffusivities obtained can be used in drying simulators for the optimization of the process. That is, to find the drying conditions such that cocoa beans with upper limits of moisture and acidity concentrations can be obtained with minimal energy consumption.

Acknowledgement

The authors express their acknowledge to Mexican Dirección General de Educación Superior Tecnológica (DGEST) for the financial support through the Project 2192.09-P.

Appendix A

A.1. Qualitative analytical solution of any parabolic equation in an orthogonal basis

Non-steady diffusive equation is a parabolic differential equation in partial derivatives, which describes the variation of concentration in a dominium (Ω) as function of time. Assuming a constant average diffusivity the non-steady diffusive equation can be written as,

$$\frac{\partial \Psi}{\partial \tau} = \nabla^2 \Psi \quad \text{in } \Omega \text{ and } \tau \geqslant 0 \tag{A.1}$$

where

$$\Psi = \frac{X - X_e}{X_0 - X_e}, \quad \tau = \frac{D_\Omega t}{l^2} (\text{Fourier number})$$

and Ω is the space dominium in which the diffusion occurs. At the boundary of the dominium S_Ω convective mass transfer occurs to or from another dominium. That is, the boundary conditions were defined by Eqs. (3) to (5),

$$-\mathbf{n} \cdot \nabla \Psi = Bi_m \Psi \text{ at } S_\Omega \tag{A.2}$$

where mass Bi number was defined as, $Bi_m = \frac{k_c l}{D_\Omega}$. In the case that $Bi_m \gg 1$, which means that the drying was controlled by diffusion, the boundary conditions becomes,

$$\Psi = 0 \text{ at } S_\Omega \tag{A.3}$$

Traditionally, Eq. (A.1) has been solved assuming the temperature as constant. However, in a typical drying process exist initial stages in which the temperature is not constant; therefore the initial con-

dition of Eq. (A.1) is the concentration profiles at the end of the variable temperature stage. That is,

$$\Psi = f_0(\Omega) \quad \text{at } \tau = \tau_0 \tag{A.4}$$

where τ_0 is the Fourier number in which the temperature has reached the equilibrium. If the dominium (Ω) is represented by orthogonal coordinate system, Eq. (A.1) can be solved by variable separation,

$$\Psi = T(\tau)O(\Omega) \tag{A.5}$$

The function $O(\Omega)$ must be separated as function of individual coordinates. Therefore Eq. (A1) can be written as,

$$\frac{1}{T(\tau)}\frac{\partial T(\tau)}{\partial \tau} = \frac{1}{O(\Omega)}\nabla^2 O(\Omega) = -\lambda^2 \tag{A.6}$$

The time function can be easily solved to give,

$$T(\tau) = C_1 e^{-\lambda^2 \tau} \tag{A.7}$$

The space differential equation,

$$\nabla^2 O(\Omega) = -\lambda^2 O(\Omega) \tag{A.8}$$

can be divided in individual differential equations for each of the coordinates used to describe the dominium, which are Sturm–Liouville problems (Wylie, 1951). That is, second order differential equations with defined boundary conditions. Therefore, individual λ^2 for each one of the Sturm–Liouville problems are the eigenvalues for which the solution satisfies the differential equation and boundary conditions. A general solution of this problem is,

$$O(\Omega) = \sum_{k=1}^{\infty}\sum_{j=1}^{\infty}\sum_{i=1}^{\infty} C_{kji} fe_1(\lambda_{1kji}, \Omega_1) fe_2(\lambda_{2kji}, \Omega_2) fe_3(\lambda_{3kji}, \Omega_3) \tag{A.9}$$

In Eq. (A.8) $fe_n(\lambda_{nkji}, \Omega_n)$ represent mathematical functions that solve individual Sturm–Liouville problems for any orthogonal coordinate Ω_n, and with the eigenvalue λ_n. The referred functions that may be either single or linear combination of sin, cos, any kind of Bessel functions, Legendre polynomials, Mathieu functions in the case of elliptic coordinates (Gutiérrez-Vega et al., 2003), or others, in agreement with the orthogonal coordinate system used. Under boundary conditions (A.2) λ_n depend only of the nature of coordinate system and the size of the medium, and under orthogonal coordinate system λ^2 (Eqs. (A6) and (A7)) is a linear combination of λ_n^2. Eq. (A9) represents the solution when the three space directions (3D) are required. Many mass transfer problems can be reduced to a 2D or 1D, keeping the mathematical nature of Eq. (A.8). Therefore without lost of generality the solution of Eq. (A.1) may be expressed as,

$$\Psi = \sum_{i=1}^{\infty} C_i fe_1(\lambda_{1i}, \Omega_1) e^{-\lambda_{1i}^2 \tau} \tag{A.10}$$

The last constant was obtained from initial conditions (A.3), and the properties of a Sturm–Liouville problem,

$$C_i = \frac{\int_{\Omega_1} f_0(\Omega_1) w(\Omega_1) fe_1(\lambda_{1i}, \Omega_1) d\Omega_1}{e^{-\lambda_{1i}^2 \tau_0} \int_{\Omega_1} w(\Omega_1) fe_1^2(\lambda_i, \Omega_1) d\Omega_1} \tag{A.11}$$

Where $w(\Omega_1)$ is the weight function of Sturm–Liouville problems (Wylie, 1951). Finally, the average dimensionless concentration is obtained by integration of Eq. (A.9) over the dominium, which gives,

$$\bar{\Psi} = \sum_{i=1}^{\infty} K_i e^{-\lambda_{1i}^2 \tau} \tag{A.12}$$

with the constant defined as,

$$K_i = C_i \int_{\Omega_1} h(\Omega_1) fe_1(\lambda_{1i}, \Omega_1) d\Omega_1 \tag{A.13}$$

and $h(\Omega_1)$ is the scale factor of the coordinate system. When the Fourier number (τ) is greater than a given value, the high terms of the series are neglected and the solution reaches its asymptotic form,

$$\bar{\Psi} = K_1 e^{-\lambda_{11}^2 \tau} \tag{A.14}$$

The slope of Eq. (A.13) in a semi-log scale is $-\lambda_{11}^2$ which depend only of the type of orthogonal coordinate system used and the size of the dominium. The effect of variable temperature at the initial stage of the process is taken into account in constant K_1 as it is shown in Eqs. (A.10) and (A.12).

References

Augier, F., Nganhou, J., Benet, J.C., Berthomieu, G., Barel, M., 1999. Experimental study of matter transfer in cocoa beans during fermentation and drying. Drying Technology 17 (6), 1027–1042.

Bird, R.B., Steward, W.E., Lightfoot, E.N., 1960. Transport Phenomena. Wiley, New York.

Brito, E.S., Pezoa-García, N.H., Gallao, M.I., Cortelazzo, A.L., Fevereiro, P.S., Braga, M.R., 2000. Structural and chemical changes in cocoa (*Theobroma cacao* L.) during fermentation, drying and roasting. Journal of the Science of Food and Agriculture 81, 281–288.

Crank, J., 1975. The Mathematics of Diffusion. Clarendon Press, Oxford.

Faborode, M.O., Favier, J.F., Ajayi, O.A., 1995. On the effects of forced air drying on cocoa quality. Journal of Food Engineering 25, 455–472.

García-Alamilla, P., Salgado-Cervantes, M.A., Barel, M., Berthomieu, G., Rodriguez-Jimenes, G.C., García-Alvarado, M.A., 2007. Moisture, acidity and temperature evolution during cacao drying. Journal of Food Engineering 79, 1159–1165.

Gutiérrez-Vega, J.C., Rodríguez-Dagnino, R.M., Meneses-Nava, M.A., Chávez-Cerda, S., 2003. Mathieu functions, a visual approach. American Journal of Physics 71, 233–242.

Hernández-Díaz, W.N., Ruíz-López, I.I., Salgado-Cervantes, M.A., Rodríguez-Jimenes, G.C., García-Alvarado, M.A., 2008. Modeling heat and mass transfer during drying of green coffee beans using prolate spheroidal geometry. Journal of Food Engineering 86, 1–9.

Hii, C.L., Law, C.L., Cloke, M., 2009. Modeling using a new thin layer drying model and product quality of cocoa. Journal of Food Engineering 90, 191–198.

Jinap, S., Thien, J.M., Yap, T.N., 1994. Effect of drying on acidity and volatile fatty acids content of cocoa beans. Journal of the Science of Food and Agriculture 65, 67–75.

Seber, G.A.F., Wild, C.J., 1989 (Nonlinear Regression). Wiley.

Senadeera, W., Bhandari, B.R., Young, G., Wijesinghe, B., 2003. Influence of shapes of selected vegetable materials on drying kinetics during fluidized bed drying. Journal of Food Engineering 58, 277–283.

Sherwood, T.K., 1929. The drying of solids-I. Industrial and Engineering Chemistry 21, 12–16.

Wang, Z., Sun, J., Liao, X., Chen, F., Zhao, G., Wu, J., Hu, X., 2007. Mathematical modeling on hot air drying of thin layer apple pomace. Food Research International 40, 39–46.

Wylie, C.R., 1951. Advanced Engineering Mathematics. MacGraw, Hill.